Enabling Wholly Aromatic Triphenylamine-Based Polyimides to Realize Bathochromic Emission

Meng-Chang Hou, Yu-Jen Shao, Chin-Hsuan Lin, Peng-Yi Lin, William Sun, Ying-Yi Tsai, Pi-Tai Chou, Tianle Gao, Toshifumi Satoh,* and Guey-Sheng Liou**

Meng-Chang Hou, Yu-Jen Shao, Chin-Hsuan Lin, Peng-Yi Lin, William Sun, Guey-Sheng Liou
Institute of Polymer Science and Engineering
National Taiwan University, Taipei 10617, Taiwan
E-mail: gsliou@ntu.edu.tw (ORCID: 0000-0003-3725-3768)

Ying-Yi Tsai, Pi-Tai Chou
Department of Chemistry, Taipei 10617, Taiwan
E-mail: chop@ntu.edu.tw (ORCID: 0000-0002-8925-7747)

Yu-Jen Shao
Graduate School of Chemical Sciences and Engineering
Hokkaido University, Sapporo 060-8628, Japan

Tianle Gao, Toshifumi Satoh
Division of Applied Chemistry, Faculty of Engineering
Hokkaido University, Sapporo 060-8628, Japan
E-mail: satoh@eng.hokudai.ac.jp (ORCID: 0000-0001-5449-9642)

Tianle Gao, Toshifumi Satoh
List Sustainable Digital Transformation Catalyst Collaboration Research Platform (ICReDD List-PF)
Institute for Chemical Reaction Design and Discovery
Hokkaido University, Sapporo 060-8628, Japan

Toshifumi Satoh
Department of Chemical & Materials Engineering
National Central University, Taoyuan 320317, Taiwan

Keywords: photoluminescence, high thermal stability, triphenylamine, red emission, wholly aromatic polyimide

ABSTRACT

The development of wholly aromatic polyimides (Ar-PIs) in the field of fluorescence material has long been hindered by the charge-transfer complex (CTC) effect, typically causing weak or non-detectable fluorescence intensity. Few studies have aimed to reduce the CTC effect through molecular design, enabling Ar-PIs to exhibit blue to yellow emission in solid films with high quantum efficiency (Φ_{PL}). However, current complex molecular designs pose inherent limitations for further reducing the emission energy gap toward the orange-red regions. To address this issue, in this work, we strategically designed and synthesized a series of triphenylamine (TPA)-based fluorescence diimides with various electron-donating/extended π-conjugation pendant groups to probe their emissive behaviors and the corresponding Ar-PIs properties. Notably, along a series of new Ar-PIs, **PI-TPE**, **PI-TPPA-TPE**, and **PI-TPPA** exhibit a systematic bathochromic shift emission at 540 nm, 598 nm, and 608 nm, respectively, in the film state, where **PI-TPPA** and **PI-TPPA-TPE** fill up and realize the full-spectrum emission by utilizing the TPA architecture.

1. Introduction

Polyimides (PIs) are favored in numerous applications due to their excellent and attractive properties, such as thermal stability, processability, electrical properties, and chemical stability.[1] Their exploitations span various fields, encompassing engineering plastics,[2] low-dielectric printed circuit boards,[3] and photoresists[4]. For example, PIs are utilized in aerospace applications as structural components and thermal insulation layers due to their outstanding thermal stability and mechanical properties.[5] Recently, some research has used PI materials to apply to the Li, Na, K, or Mg-ion batteries as anodic/cathodic and separator materials due to the high polarity imide ring and ample scope for designing molecules, realizing high-performance battery properties.[6] In contrast, research on luminescent applications of PIs is still limited, although their corresponding monomeric congener, such as perylene diimide, has been exploited as laser dyes[7]. Photoluminescent (PL) applications typically require high quantum-efficiency (Φ_{PL}) materials to ensure efficient energy conversion for emissive performance. Aside from Φ_{PL}, emission color is also essential, especially for the white-light display application. Unfortunately, for the wholly aromatic polyimides (Ar-PIs), whose stability is beneficial for practical applications, the formation of charge transfer complexes (CTCs) often results in poor emission performance.[8] CTC includes two types of charge transfers (CT): (i) intermolecular CT caused by the well-packing PI chains and (ii) intramolecular CT induced by adjacent diamine moieties as donors and dianhydride moieties as acceptors. Both CT effects make conventional Ar-PIs films weakly emissive and limited in blue-to-yellow regions. Overcoming or ameliorating their intrinsic CTC formation is thus crucial and an ongoing issue.[9] For example, Hasegawa and Horie conducted extensive research on the formation and effects of CTC in PIs, reporting that general Ar-PIs films exhibit CT fluorescence and show extremely low Φ_{PL}.[8] To enhance the emissive behaviors of PIs, Ando *et al.* systematically investigated the structure-fluorescence relationship of the PIs by combining theoretical calculations and experimental results. They proposed an effective method to reduce inter- and intramolecular CT by incorporating alicyclic diamine and flexible ether linkages in the dianhydride moiety. As a result, the semi-aromatic PIs (Al-PIs) were prepared, achieving a film-state Φ_{PL} of 11%.[10] Recently, studies have demonstrated that incorporating aggregation-induced emission luminogen (AIEgen) and alicyclic linkages enables PIs to attain considerable film-state Φ_{PL}. Our previous report on Al-PIs using 4-cyanotriphenylamine-based diamine as an AIEgen and an alicyclic dianhydride moiety resulted in a film-state Φ_{PL} of 65%.[11] Zhang *et al.* reported triphenylethylene-based AIEgen with alicyclic dianhydride moiety to obtain a

high Φ_{PL} Al-PI in film-state up to 89%.[12] Hence, incorporating AIEgens or alicyclic moiety in PIs becomes a practical and common way to prepare high Φ_{PL} films.[13]

Although the alicyclic bond effectively reduces the CTC effect and thereby increases the emissivity, Al-PIs commonly sacrifice their excellent thermal properties at the same time.[10, 14] To address this issue, our previous works found that using triphenylamine (TPA)-based dianhydride luminophores was an effective and judicious strategy for designing highly emissive Ar-PI films while simultaneously preserving thermal properties. This intriguing PL behavior is due to the electron-donating TPA unit effectively reducing the electron-withdrawing ability of the anhydride moieties, suppressing intramolecular CT within the Ar-PI backbone.[14a, 14b, 15] We then reported on a series of Ar-PIs with high Φ_{PL} by combining TPA-based dianhydride with twisted and bulky moieties that can prevent dense chain packing. Among the resulting Ar-PIs, the naphthalene pendant group exhibits the highest Φ_{PL} of 22% in the film state.[15b] In a subsequent study, a series of Ar-PIs derived from TPA-based dianhydride and other *p*-phenylenediamines containing various numbers of methyl groups were designed by introducing multi-methyl substituents in the dianhydride and diamine moieties generating a highly twisted conformation between the diamine and dianhydride moieties,[14a] which effectively suppresses intra and intermolecular CT, exhibiting high Φ_{PL}. As a result, the film state Φ_{PL} rises from 35% without methyl groups in the diamine moiety (**PI3M-0M**) to 61% in the tetramethyl one (**PI3M-4M**). At the same time, this series of Ar-PIs also demonstrates high T_g, among which T_g of **PI3M-4M** can reach as high as 470 ℃.

The abovementioned reports have displayed various Al- or Ar-PIs with high Φ_{PL}. Unfortunately, their emission colors are usually limited to blue to greenish-yellow. Thus, developing more extended and red-shifted emissive PIs is essential and urgent, which is challenging.[16] Reports have shown that introducing polycyclic aromatic hydrocarbons (PAHs) like perylene into the semi-aromatic system can achieve red emission in solution.[17] However, these rigid and highly coplanar structures often result in aggregation-caused quenching (ACQ) behavior, revealing none or weak emissive behavior in the film state.[16e, 18] Ando et al. designed a series of semi-aromatic PIs with hydroxyl groups modified on the dianhydride moieties to achieve longer emission wavelengths so that excited-state intramolecular proton transfer (ESIPT) can occur.[19] Among them, **3H-PI** exhibits a noticeable orange-red emission at 590 nm with Φ_{PL} of 6.8% in the film state. However, these red-emitting PIs are based on semi-aromatic moieties, resulting in a reduction of thermal properties.

In this work, we report a series of new full aromatic Ar-PIs, which successfully demonstrate intense red emission and excellent thermal stability. Four TPA-architecture

diimide compounds were designed and synthesized according to two strategies: (i) We incorporate the electron-donating methoxy group at the *para* position of the phenyl ring or 4,4′-dimethoxy diphenylamine group to the TPA-diimide, generating a strong donor-acceptor structure. (ii) We introduce the AIE-active triphenylethylene (TPE) at the *para* position of the phenyl moiety within the TPA-diimide to induce red-shifted emission through the extended π-conjugation, preventing π-π stacking and hence ACQ in the film state (see **Scheme 1**). Among them, **PI-TPA** and **PI-TPE** exhibited remarkable film-state Φ_{PL} values of 23% and 47%, respectively, with yellowish emission. In particular, **PI-TPPA** and **PI-TPPA-TPE** demonstrated noticeable orange-red emission at 608 nm and 598 nm in the film state while preserving outstanding thermal stability with T_g values up to 365 and 325 °C, respectively.

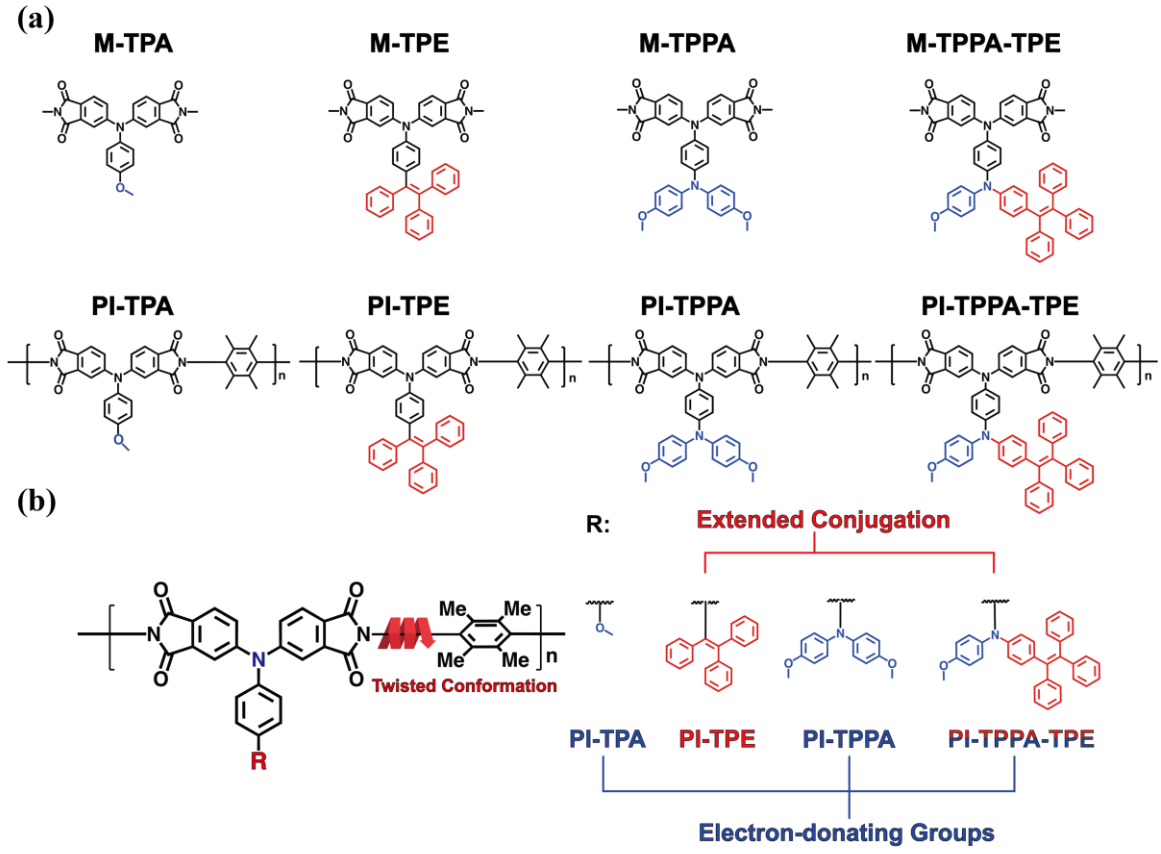

Scheme 1. (a) Chemical structures of all observed model compounds and polyimides. (b) The design concept for bathochromic emission in TPA-based Ar-PIs.

2. Results and Discussion

2.1. Synthesis, characterization, and photophysical properties

The new series of diimide compounds with different electron-donating or withdrawing pendant groups were successfully synthesized through the Buchwald–Hartwig amination reaction to probe the photophysical properties systematically.[14a, 14b, 15b, 20] Synthetic routes are summarized in **Schemes S1-S2**, and detailed preparation procedures are depicted in the Supporting Information. All diimide model compound structures were confirmed by FT–IR, ^{1}H, ^{13}C, ^{1}H–^{1}H COSY, and ^{13}C–^{1}H HSQC NMR spectra (**Figures S1–S17**). In **Figure S1**, all diimide model compounds showed imide ring C=O symmetric and asymmetric stretching peaks around 1710 and 1770 cm^{-1}, respectively, and confirmed no primary or secondary amine stretching peaks in the 3300-3500 cm^{-1} range. The photophysical properties of these model compounds were measured by PL and UV-vis spectra, as demonstrated in **Figures 1a,b** and **S18a,b** and tabulated in **Table 1**. All the model compounds exhibited a characteristic absorption peak around 420 to 440 nm in both solid and solution states. These peaks could be attributed to the characteristic of hybridized local-charge transfer (HLCT) absorption, involving locally excited (LE) π–π* transition and intramolecular CT π–π* transition between the electron-accepting phthalic imide and the electron-donating arylamine moiety.[14a, 14b, 21] The HLCT excitation peaks could also be found in the PL excitation spectra in both solid and solution states, as illustrated in **Figures S19-S20**. The non-substitution at the *para* position TPA diimide (**M-TPA-H**) exhibited green fluorescence at 512 nm in the solid state. [14a] Upon extending the conjugation length by triphenylethylene building block, **M-TPE** exhibited a bathochromic emission to 542 nm and a solid-state Φ_{PL} of 22.1%.

Table 1. Photophysical properties of diimide compounds in the solution and the solid states and photographs under room light and UV-365 nm irradiation in the solid state.

Code	λ_{max}^{abs} [nm]	λ_{max}^{em} [nm] [a]	Φ_{PL} [%] [b]	λ_{max}^{abs} [nm]	λ_{max}^{em} [nm] [a]	ν [cm^{-1}] [c]	Φ_{PL} [%] [d]	α_{AIE} [e]	Room light	UV-365
	Solution [d]			Solid						
M-TPA	422	550	8.2	423	558	5720	39.6	4.8	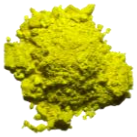	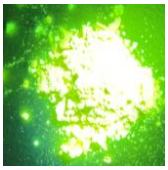
M-TPE	430	542	2.9	422	542	5246	22.1	7.6		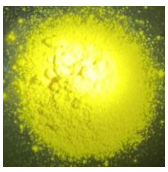
M-TPPA	441	598	0.1	430	610	6862	1.6	16.0		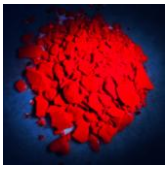
M-TPPA-TPE	437	597	0.1	425	593	6666	1.3	13.0		

[a] λ_{max}^{em} were excited at λ_{max}^{abs}.

[b] The quantum yield was measured using quinine sulfate (dissolved in 1 N H_2SO_4 with a concentration of 10 μM, assuming its Φ_{PL} = 0.546) as a standard at 25 °C.

[c] Stokes shift was calculated by equation $\nu = 10^7 \times \left(\frac{1}{\lambda_{max}^{abs}} - \frac{1}{\lambda_{max}^{em}}\right)$.

[d] Φ_{PL} in the solid state was determined using a calibrated integrating sphere.

[e] Calculated by the equation $\alpha_{AIE} = \frac{\Phi_{PL(Solid)}}{\Phi_{PL(Solution)}}$.

[f] Solution state was measured in chloroform (concentration 10 μM).

Meanwhile, the methoxy-substituted M-TPA displayed a further bathochromic emission to 558 nm and gained a high solid-state Φ_{PL} of 36.9%, implying that extending conjugation or introducing electron-donating substitutions is beneficial to the induction of red-shifted emission, where the latter seems to show better effectiveness as well as higher solid-state Φ_{PL}. Accordingly, more substantial electron-donating groups or building blocks in the TPA

architecture are expected to develop further red-shifted Ar-PIs emitter. This concept was supported by **M-TPPA**, in which the para-methoxy-diphenylamine building block, possessing stronger electron-donating characteristics compared to the methoxy group in **M-TPA** (see **Scheme 1**), exhibited significant bathochromic emission at 610 nm in the solid state. In comparison, adding a π-extended TPE building block to replace one of the para-methoxy-phenyl arms in **M-TPPA** forms **M-TPPA-TPE** (**Scheme 1**), which reveals a blue-shifted emission at 593 nm (cf. 610 nm in **M-TPPA**) in the solid state. The results reaffirm that electron-donating strength is more crucial than extending π-conjugation in lowering the emission gap. While further bathochromic tuning is successful, **M-TPPA** and **M-TPPA-TPE** reveal low emission Φ_{PL} of 1.6% and 1.3%, respectively, in the solid state. Comparing the high emission Φ_{PL} of 22.1% for **M-TPE** (542 nm) and 36.9% for **M-TPA** (558 nm) in the green-yellowish region, the results of low emission Φ_{PL} in the red can be rationalized by the nonradiative decay rate associated with internal conversion (k_{ic}), that is expressed empirically by

$$k_{ic} \sim 10^{13} e^{-\alpha \Delta E} \quad (1)$$

where ΔE is the emission energy gap, which is unitless but could be assessed by kcal/mol, α is the positive proportionality constant (≥ 0). Therefore, k_{ic} increases as both ΔE and α decrease, aligning with the empirical energy gap law in **Equation 1**. The parameter α decreases with an increase in the reorganization energy λ. For example, polyatomic molecules possessing π-π* transition, rigid structure, and long π-conjugation commonly have small λ, and α is in an average of ~0.18.[22] k_{ic} is expected to increase significantly when ΔE decreases from green to red region. In addition, the synthesized PIs in this study all possess CT character with extensive λ, as supported by significant Stokes shift (Δν) between absorption and emission peak frequencies (see Table 1); hence, α is expected to be < 0.18 for all studied Ar-PIs. Moreover, to tune emission toward the red region, an increase of electron-donating strength, hence stronger CT character, is necessary (vide supra), resulting in a further increase of λ, i.e., a decrease of α. The more minor ΔE and α thus lead to a drastic increase of k_{ic}, rationalizing the much decrease of Φ_{PL} for **M-TPPA** and **M-TPPA-TPE**. To further investigate this, TR-PL measurements of this series of diimides were performed to calculate the emission lifetime (τ), emission decay rate (k_{obs}), and radiative and nonradiative decay rate (k_r/ k_{nr}) presented in **Figure S21** and **Table 2**. *The observed emission decay rate k_{obs} give additional support for* **M-TPA**, **M-TPE**, **M-TPPA**, and **M-TPPA-TPE**. Theoretically, Φ_{PL} is expressed by $\Phi_{PL} = k_r/k_{obs}$, where k_r is the emission radiative decay rate constant. $k_{obs} = k_r + k_{nr}$ where k_{nr} is the sum of all

nonradiative decay rates. Assuming that k_{nr} is dominated by k_{ic} in the rigid solid state, k_{ic} for **M-TPPA** and **M-TPPA-TPE** is nearly fivefold as large as that of **M-TPA** and **M-TPE**. Furthermore, k_r values of **M-TPA** and **M-TPE** are significantly higher than those of **M-TPPA** and **M-TPPA-TPE**, indicating that the stronger electron-donating groups in **M-TPA** and **M-TPE** lead to a higher k_r and a lower k_{ic}, ultimately resulting in a higher quantum yield. This observation further supports the operation of the energy gap law.

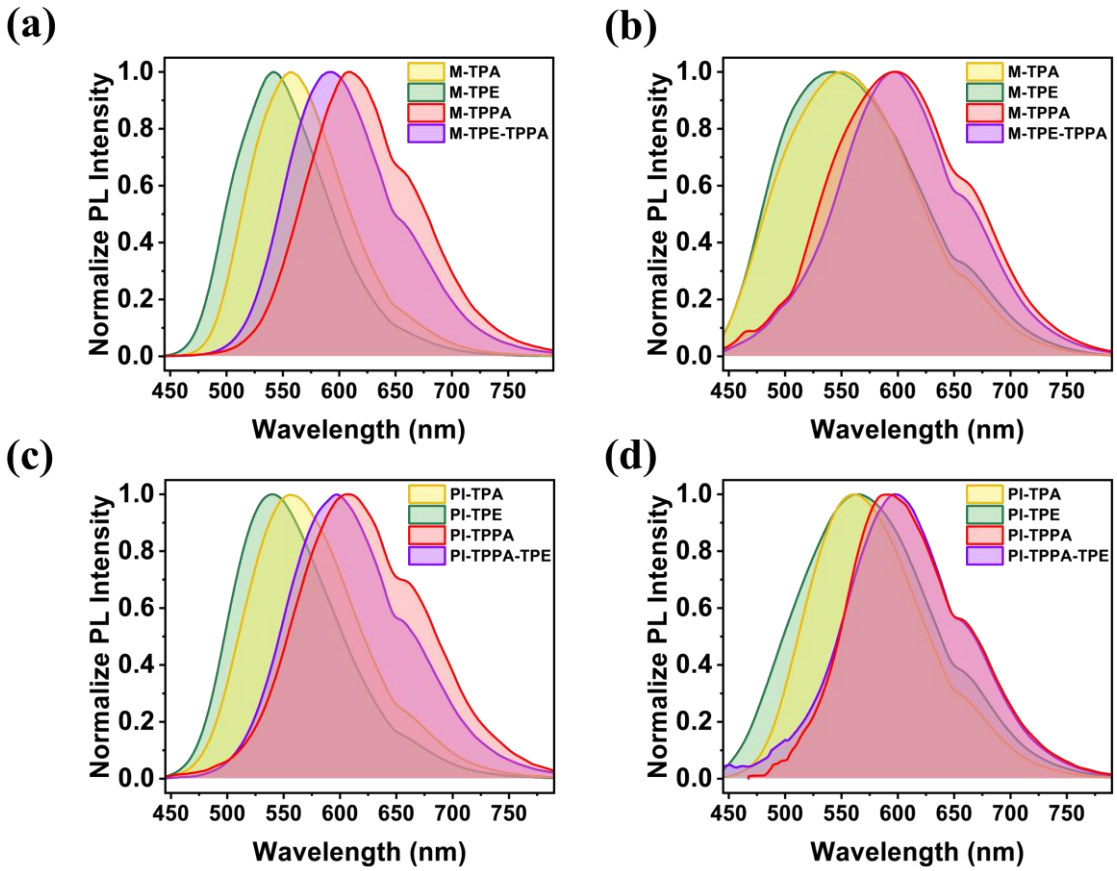

Figure 1. PL spectra of diimide model compounds and Ar-PIs under a,c) solid state, and b,d) dissolved in $CHCl_3$ with a concentration of 10 μM. All PL spectra were excitation at the maximum absorption wavelength.

Table 2. Photophysical properties, observed lifetime (τ_{obs}), observed emission decay rate constants (k_{obs}), and radiative/nonradiative rate constants (k_r/k_{nr}) of diimide compounds in the solid states.

Code	λ_{max}^{abs} [nm]	λ_{max}^{em} [nm] [a]	τ_{obs} [ns]	k_{obs} [s^{-1}] [b]	k_r [s^{-1}] [c]	k_{nr} [s^{-1}] [c]	Φ_{PL} [%] [d]
M-TPA	423	558	2.45	4.1×10^8	1.5×10^8	2.6×10^8	39.6
M-TPE	422	542	3.80	2.6×10^8	5.8×10^7	2.1×10^8	22.1
M-TPPA	430	610	0.65	1.5×10^9	2.5×10^7	1.5×10^9	1.6
M-TPPA-TPE	425	593	1.04	9.6×10^8	1.3×10^7	9.5×10^8	1.3

[a] λ_{max}^{em} were excited at λ_{max}^{abs}.

[b] Calculated by the equation $k_{obs} = k_r + k_{nr}$.

[c] Calculated by the equation $\Phi_{PL} = \tau_{obs} \times k_r = \frac{k_r}{k_r+k_{nr}}$.

[d] Φ_{PL} was determined using a calibrated integrating sphere.

To gain further insight into the impact of donating groups and π-extending building block, the time-dependent density functional theory (TD-DFT) was applied to elucidate the electron distribution, energy level, band gap (E_g in **Equation 1**), and oscillator strength (*f*). The results are shown in **Figure 2** and summarized in **Tables S1-S2**. As a comparison, the values of the optical E_g calculated through the UV-vis spectra are tabulated in **Table S3**. **Figure 2** demonstrates that the lowest unoccupied molecular orbital (LUMO) of all diimide compounds is symmetrically on the phthalic imide moieties; the energy level shifts slightly with different pendant groups. Comparatively, the distribution and corresponding energy level of the highest occupied molecular orbital (HOMO) strongly depend on the pendant groups. In the case of **M-TPA-H** and **M-TPA**, the HOMOs are across all the TPA moieties. *f* values are obtained to be as large as 0.2774 and 0.2649, respectively, supporting the hybridized local (π-π*) and charge transfer (CT) character, i.e., the aforementioned HLCT transitions.

In contrast, for **M-TPE**, **M-TPPA**, and **M-TPPA-TPE**, the HOMOs were almost only distributed on the pendant building blocks, revealing a tendency of shifting from the HLCT to the CT transition with smaller *f* values (see **Figure 2** and **Tables S1-S2**). For **M-TPA-H** and **M-TPA**, simply introducing a methoxy group at the *para* position of the phenyl ring, E_g reduced from 3.51 eV to 3.34 eV. Extending the conjugation is exemplified by comparing M-**TPA-H** and **M-TPE**, where incorporating **M-TPA-H** (E_g~3.51 eV) with a triphenylethylene moiety, E_g of **M-TPE** decreased to 3.24 eV. The results of the calculation are consistent with the

experimental observation in that using an electron-donating group and/or π-extending building block could significantly uplift the HOMO energy levels. In contrast, the LUMO energy level remains almost unchanged, leading to a smaller E_g value, hence a bathochromic absorption and emission. Calculations also show that **M-TPPA** and **M-TPPA-TPE** exhibited a much smaller E_g than **M-TPA** and **M-TPE**, with values as low as 2.79 eV and 2.78 eV, respectively. Thus, TPPA moiety, having stronger electron-donating strength than TPA, effectively reduces the E_g, resulting in a further bathochromic emission shift.

The dipole moments of the ground state (μ_g) and excited state (μ_e) for the titled compounds were also computed to gain solvatofluorochromic properties. Detailed calculation methodology and the resulting data are described in the Supporting Information (**Figures S22-S26** and **Table S4-S8**). From **Table S8**, **M-TPA** (μ_g = 5.19 D) and **M-TPE** (μ_g = 4.03 D) exhibited similar ground-state dipole moment (μ_g) values. In comparison, **M-TPA** (μ_e = 26.31 D) showed a significantly higher μ_e than **M-TPE** (μ_e = 16.24 D), indicating that introducing electron-donating groups should be more effectively than extending the conjugation length to facilitate polarization in the excited state. Meanwhile, **M-TPPA** and **M-TPPA-TPE** revealed lower Φ_{PL} values in the various organic solvents, and all the diimide compounds performed similar emission colors in the $CHCl_3$ solution but lower Φ_{PL} values correspondingly compared to the solid state (**Table 1**).

We also performed test aggregation-induced emission (AIE) by gradually adding poor solvent (water) in the THF solution to investigate the fluorescent behavior from the isolated to aggregated states, as shown in **Figures S27-S30**. In pure THF solution (as a good solvent), all the model compounds exhibited weak emission intensity and low Φ_{PL}, attributed to numerous free rotors in the structure, undergoing nonradiative dissipation via rotations in the solution state. A slight decrease in PL intensity could be observed when increasing the water (as a poor solvent) fraction (f_w) to 10% due to the protonation of water and the twisted intramolecular charge transfer (TICT) effect.[23] Subsequently, as f_w increased at around 50%–70%, the nanoparticles started generating a prominent PL intensity increment caused by the restriction of the intermolecular motions (RIMs) of AIE, demonstrating that all the diimide compounds can be classified as the AIE luminophores (**Figure S31**).[24] In particular, **M-TPPA-TPE** performs more AIE-active characteristics with the most significant relative emission intensity ratio of 77.2-fold.

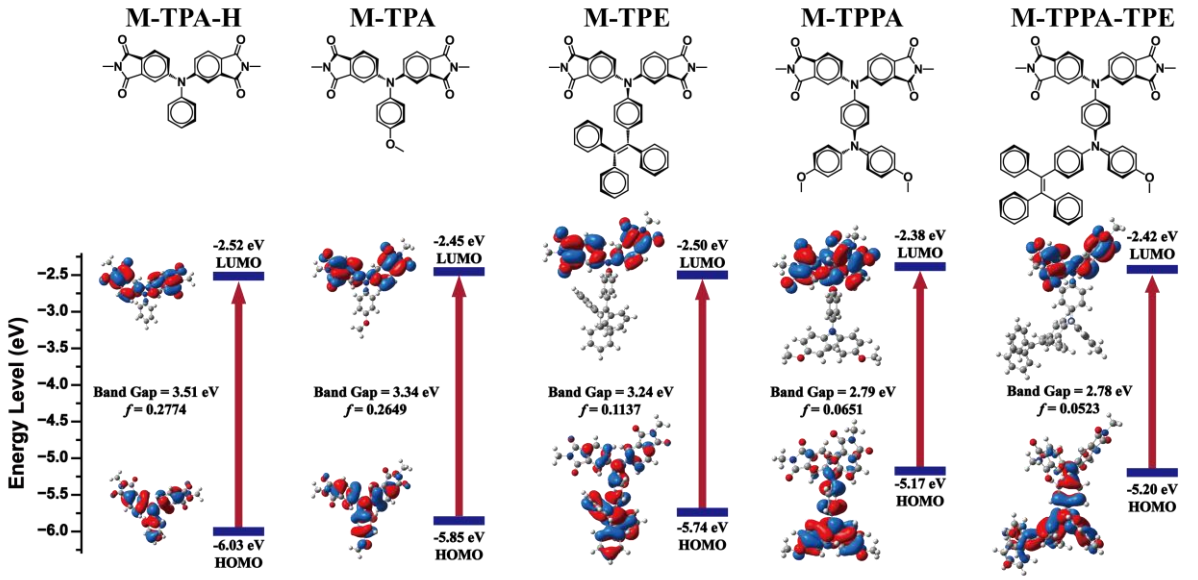

Figure 2. Molecular simulation results of diimide model compounds with TD-DFT method at the B3LYP/6-311G (d,p).

2.2. Basic Properties and Thermal Properties of Polyimides

In order to explore the photophysical behaviors of the corresponding Ar-PIs, all diimide compounds are synthesized into dianhydrides by hydrolysis and cyclodehydration reactions, as described in our earlier research.[14a, 14b, 15b, 20] Next, these dianhydrides are polymerized with 2,3,5,6-tetramethyl-*p*-phenylenediamine in *m*-cresol or NMP at 180 °C via the one-step imidization to yield a series of fluorescent Ar-PIs. Detailed synthetic and purification procedures are elaborated in the Supporting Information. The structures of dianhydride compounds and Ar-PIs were confirmed by FTIR (**Figure S32–S33**) and ^{1}H–NMR (**Figures S34–S41**). In **Figure S32**, the dianhydride compounds showed anhydride C=O symmetric and asymmetric stretching peaks around 1770 and 1840 cm^{-1}. After polymerization, the anhydride stretching peaks disappeared, and imide ring C=O symmetric and asymmetric stretching peaks appeared around 1720 and 1770 cm^{-1} (**Figure S33**). The elemental analysis data of the dianhydride compounds also demonstrate their purity, enabling the preparation of Ar-PIs with high inherent viscosity and molecular weight from 0.36 – 0.77 dL/g and 12.9 – 64.3 kDa, as tabulated in **Tables S9** and **S10**. In the same table, the prepared Ar-PIs were well dissolved in various organic solvents, even in low-polarity solvents like chloroform, THF, or DCM, manifesting excellent processability. Thus, we could also prepare the free-standing, flexible, and transparent films through simple drop or blade coating, as shown in **Table 3** and **Figures 3d** and **3e**. In TGA and TMA measurements (**Figure 3a, 3b**, and **Table S11**), all the resulting Ar-PIs exhibited excellent thermal stability and glassy transition temperature (T_g). For example, due to the high aromatic content, rigid backbone, and smaller methoxy pendant group, PI-TPA

revealed the highest T_g at 435 °C. As bulky pendant building blocks like diphenylamine or TPE were introduced, the free volume increased in the structure, and T_g decreased. Nevertheless, this series of Ar-PIs maintained the T_g values above 325 °C and exhibited the decomposition at 5 wt% loss temperatures (T_d^5) above 455 °C owing to the wholly aromatic structure.

2.3. Optical Behavior of Polyimides

The optical properties of the Ar-PIs were measured by UV-vis and PL spectroscopies, with the results presented in **Figures 1c,1d, S18c**, and **18d** and summarized in **Table 3**. Like the M-series model compounds (vide supra), all Ar-PIs exhibited, to a certain extent, an HLCT absorption peak around 420 to 440 nm in both solid and solution states. PL excitation spectra in **Figures S42-S43** also showed corresponding HLCT excitation peaks. The AIE test was applied to observe the aggregate state of the resulting Ar-PIs from the isolated state, as depicted in **Figures S44–S48**. In the case of **PI-TPA** and **PI-TPE**, since the twisted diamine moiety could fix the molecular chain and TPA and TPE diimide moieties were the strong fluorophore as afore-studied, these two Ar-PIs exhibited delectable and noticeable emission intensity in the pure THF solution. Upon adding the water fraction (f_w) to THF up to 10%, **PI-TPA** and **PI-TPE** exhibit a slight decrease in PL intensity, probably caused by water protonation and the TICT effect.[23] Subsequently, along with the f_w increased to around 70%–90%, the formation of nanoparticles starts to be observed, which restricts intramolecular motions (RIMs) of Ar-PIs, resulting in a dramatic increase in PL intensity.[24] Therefore, **PI-TPA** and **PI-TPE** could be regarded as aggregation-induced emission enhancement (AIEE) characteristics. On the contrary, **PI-TPPA** and **PI-TPPA-TPE** showed relatively poor emission intensity in pure THF solution. As f_w increased to around 70%–90%, the PL intensities could enhance 12.5-fold and 18.1-fold for **PI-TPPA** and **PI-TPPA-TPE**, respectively. Hence, **PI-TPPA** and **PI-TPPA-TPE** could be regarded as polymers having AIE characteristics.

In the film state, with the help of the highly twisted diamine moiety, the resulting Ar-PIs displayed similar emission colors with the corresponding diimide compounds. Also, they preserved the Φ_{PL}, as shown in **Table 3**. **PI-TPA** (558 nm) exhibited a longer emission wavelength than **PI-TPE** (540 nm) in the film state. At the same time, **PI-TPE** (Φ_{PL} = 47.4%) revealed higher film-state Φ_{PL} than **PI-TPA** (Φ_{PL} = 23.0%) due to the bulky TPE pendant group preventing intermolecular charge transfer. Notably, **PI-TPPA-TPE** and **PI-TPPA** manifested the orange (598 nm) and red (608 nm) emission colors under UV-365 nm irradiation, filling the gap at the longer wavelength of panchromatic emission region for TPA-based Ar-PIs, as depicted in **Figure 3c**. Additionally, the film-state emission lifetime profiles also indicated that

the k_r values of **PI-TPA** and **PI-TPE** are higher than those of **PI-TPPA** and **PI-TPPA-TPE**, echoing the results from the model compounds, as shown in **Figure S49** and **Table S12**. In order to address the effect of pendant groups on the emission color more clearly, the emission CIE 1931 color coordinates of the Ar-PIs are presented in **Figure 4** and summarized in **Table 4**. The color coordinate distance was calculated using **PI-TPA-H** without substituent groups as the reference point. When comparing distances, **PI-TPA** (distance = 98) indicated a much more extended shift than **PI-TPE** (distance = 51), proving again that the electron-donating group could more beneficially facilitate a bathochromic emission color.

Table 3. Optical properties of Ar-PIs and photographs under room light and UV-365 irradiation in the film state.

Code	λ_{max}^{abs} [nm]	λ_{max}^{em} [nm] [a]	Φ_{PL} [%] [b]	λ_{max}^{abs} [nm]	λ_{max}^{em} [nm] [a]	ν [cm^{-1}] [c]	Φ_{PL} [%] [d]	α_{AIE} [e]	Room light	UV-365
	Solution [f]			Solid						
PI-TPA	423	561	12.0	422	558	5776	23.0	1.91		
PI-TPE	406	564	5.3	410	540	5872	47.4	8.83	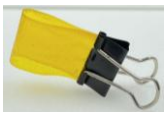	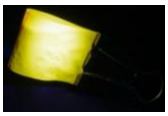
PI-TPPA	433	591	0.7	430	608	6808	1.04	1.48		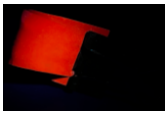
PI-TPPA-TPE	435	598	0.8	425	598	6807	1.13	1.41		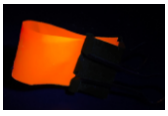

[a] λ_{max}^{em} were excited at λ_{max}^{abs}.

[b] The quantum yield was measured using quinine sulfate (dissolved in 1 N H_2SO_4 with a concentration of 10 μM, assuming its Φ_{PL} = 0.546) as a standard at 25 °C.

[c] Stokes shift was calculated by equation $\nu = 10^7 \times \left(\frac{1}{\lambda_{max}^{abs}} - \frac{1}{\lambda_{max}^{em}}\right)$.

[d] Φ_{PL} in the solid state was determined using a calibrated integrating sphere.

[e] Calculated by the equation $\alpha_{AIE} = \frac{\Phi_{PL(Solid)}}{\Phi_{PL(Solution)}}$.

[f] Solution state was measured in chloroform (concentration 10 μM).

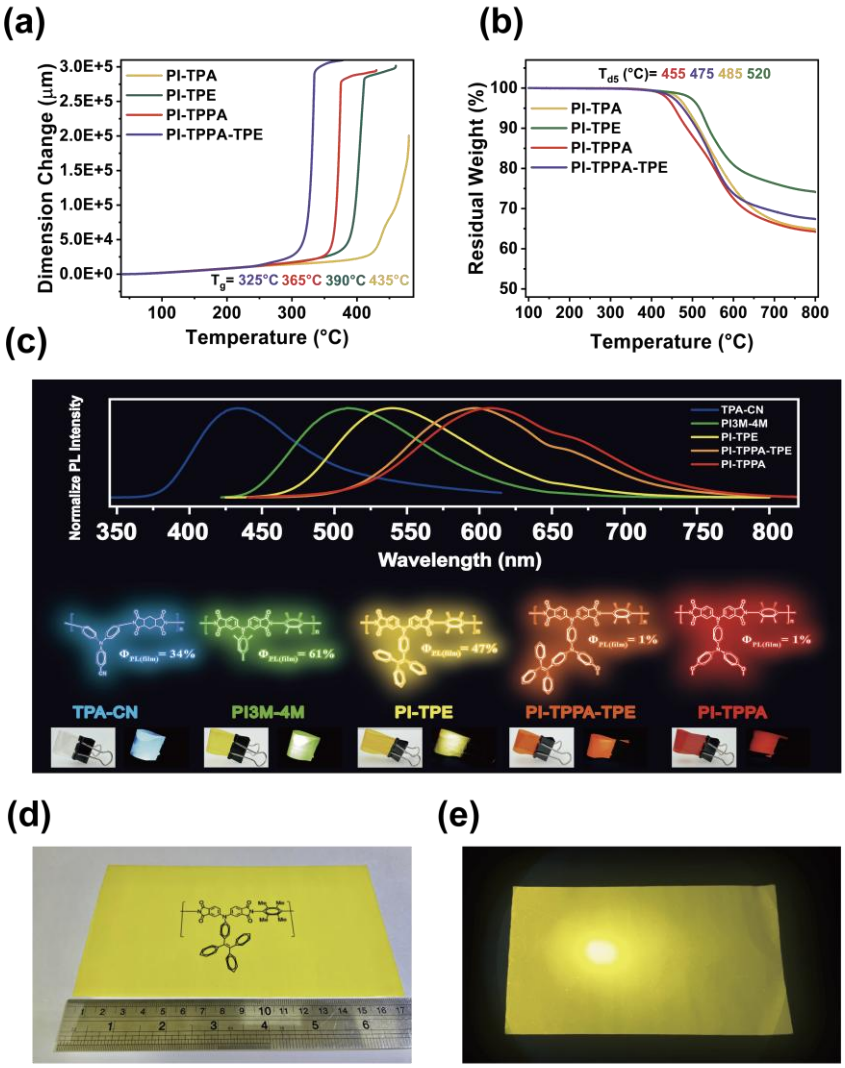

Figure 3. a) TMA and b) TGA thermograms of Ar-PIs c) Normalized emission spectra of a series of fluorescent PIs try to achieve whole-spectrum emission and their relative photographs under room light and UV-365 irradiation. Photographs of PI-TPE big film with an area of 9.5 × 17.5 cm^2 and thickness of *ca.* 7±3 μm under d) room light and e) UV-365 irradiation.

Additionally, introducing the more substantial electron-donating 4,4'-dimethoxy diphenylamine pendant group in **PI-TPPA** brings about an even more significant shift for a distance of 263 than **PI-TPPA-TPE** of 238. In the case of **PI-TPPA-TPE**, the extended conjugation from **TPE** moiety gives rise to a slightly blue-shifted emission, possibly because TPE could be considered a weak electron acceptor, thus reducing the electron-donating capability of the pendant groups. As shown in **Figure 3c**, our previous works have reported TPA-containing PIs behaving blue and green emissions with high Φ_{PL} in the film state.[11, 14a] In this study, by modifying the pendant groups of TPA-based dianhydride, we successfully

achieved the emission color tuning of Ar-PIs from yellow to red, attaining the challenging research goal of panchromatic emission in the wholly aromatic polyimide film state.

Table S13 collects and summarizes the fluorescence properties and T_g values from the previous references for Ar or Al-PIs for comparison. We could not almost notice the results on Ar-PIs films with yellow or red emissions. For those of the solid-state emission wavelength from 530 to 570 nm, the listed Al-PIs showed the solid-state Φ_{PL} of 29.0% and 14.5 % with the T_g of 331 and 317 ℃, respectively, and the Ar-PIs only revealed lower solid-state Φ_{PL} than 3% with lower T_g than 275 ℃.[12-13, 25] On the contrary, in this work, **PI-TPA** and **PI-TPE** exhibit yellow emission at 558 nm and 540 nm with remarkably high Φ_{PL} of 23.0% and 47.4% in the film state and also maintain outstanding high T_g of 435 and 390 °C, respectively. In addition, for those of the solid-state emission wavelength longer than 570 nm, the reported Al-PIs could only achieve solid-state Φ_{PL} up to 6.8%, but without the T_g value in the references.[19b, 19c, 26] To our best knowledge, only one reported Ar-PI showed an emission wavelength of 585 nm with Φ_{PL} of 1.7%. Still, it also indicates a low T_g value of only 245 ℃ owing to multi-flexible ether linkages and bulky pendant groups.[27] Although **PI-TPPA** and **PI-TPPA-TPE** exhibit a slightly lower Φ_{PL} of 1.04% and 1.13% at more red-shifted 608 and 598 nm, respectively, they display high T_g values of 365 and 325 °C. By judiciously designing TPA architectures, we thus successfully demonstrate a series of Ar-PIs with bathochromic emission colors and high T_g simultaneously to accomplish the panchromatic emission research goal of the Ar-PI film system.

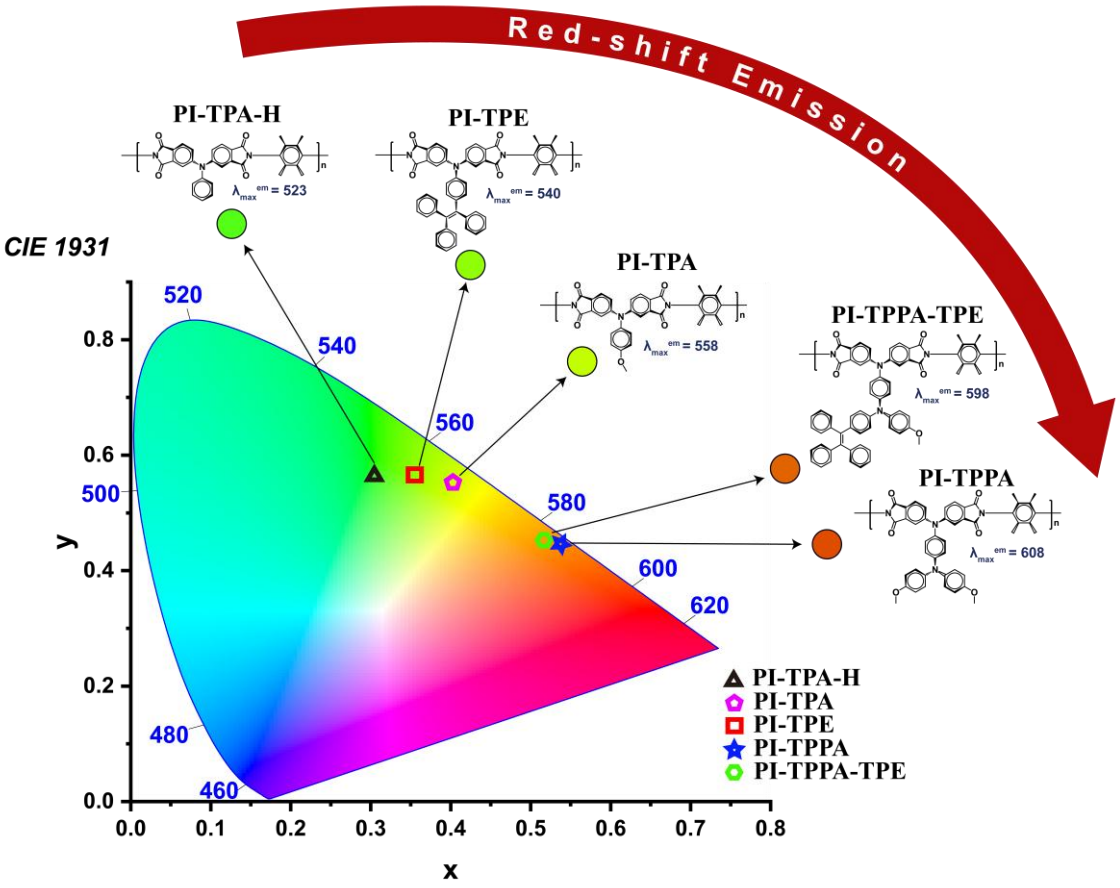

Figure 4. CIE1931 coordinates in the solid state of Ar-PIs.

Table 4. PL properties and emission CIE 1931 color coordinates of Ar-PIs in film state.

Code	λ_{max}^{abs} [nm]	λ_{max}^{em} [nm] [a]	CIE 1931 [b]		
			x	y	Distance [1×10^{-3}] [c]
PI-TPA-H	408	523	0.30479	0.56439	0
PI-TPA	422	558	0.40284	0.55279	98.73
PI-TPE	410	540	0.35582	0.56641	51.06
PI-TPPA	430	608	0.53893	0.44328	263.60
PI-TPPA-TPE	425	598	0.51604	0.45448	238.13

[a] λ_{max}^{em} was excited at λ_{max}^{abs}.

[b] CIE 1931 coordinate calculated by PL spectrum.

[c] Distance Calculated by the equation: $\sqrt[2]{(x_1-x_2)^2+(y_1-y_2)^2}$, PI-TPA-H as x_1 and y_1.

3. Conclusion

This work successfully designed and synthesized a series of fluorescent Ar-PIs with remarkably red-shifted emission and outstanding Φ_{PL} in the solid state. The effects of electron-donating pendant groups and extended π-conjugation approaches on the bathochromic emission were investigated through the optical measurements and simulations of diimide model compounds. Furthermore, the resulting corresponding Ar-PIs of **PI-TPA** and **PI-TPE** demonstrate that introducing electron-donating groups and extended conjugation should be beneficial and practical approaches to facilitate inducing bathochromic emission while maintaining higher Φ_{PL}. **PI-TPPA** and **PI-TPPA-TPE**, with the TPPA architecture, reveal reddish emissive color by merging electron-donating groups and extended conjugation approaches, enabling the Ar-PIs to demonstrate red emissive with specific film-sate Φ_{PL} values. Importantly and practically, the resulting Ar-PIs preserve high Tg and decomposition temperatures simultaneously.

4. Experimental Section

Materials

N-Methyl-4-bromophthalimide,[15b] 4-tetraphenylethenylamine,[28] 4-amino-4′,4″-dimethoxytriphenylamine,[29] and 4-methoxy-4′-nitrodiphenylamine were prepared as previous report.[30] Commercially available chemical reagents, including 4-iodoanisole (ACROS), 4-nitroaniline (ACROS), benzophenone (Alfa Aesar), titanium (IV) chloride (SHOWA), zinc dust (ACROS), Copper (II) nitrate trihydrate (SHOWA), acetic anhydride (ECHO), diphenylmethane (Alfa Aesar), 4-bromobenzophenone (Alfa Aesar), *N*-butyllithium (*n*-BuLi) (2.0M in hexane) (ACROS), *p*-toluenesuflonic acid monohydrate (ACROS), palladium (10% on carbon) (ACROS), hydrazine monohydrate (Alfa Aesar), palladium (II) acetate (UR), (±)-2,2′-bis(diphenylphosphine)-1,1′-binaphthalene (rac-BINAP) (Alfa Aesar), cesium carbonate (Alfa Aesar), tris(dibenzylideneacetone)di-palladium(0) ($Pd_2(dba)_3$) (ACROS), tri-tert-butyl phosphonium tetrafluoroborate ($HP^tBu_3BF_4$), sodium tert-butoxide (ACROS), 2,3,5,6-tetramethyl-*p*-phenylenediamine (TCI) where purified before polymerization by recrystallization, *N*-methyl-2-pyrrolidone (NMP), toluene and xylene were dry by distillation under reduced pressure over calcium hydride before used, tetrahydrofuran (THF) were dry by reflux with benzophenone and sodium for 12 hours and distillation.

Preparation of the Ar-PIs Films

For photographs, TGA, and TMA measurement, 40 mg of Ar-PIs was dissolved in 3 mL of DMF, then the solution was slowly dropped onto a 2.5×7.5 cm^2 glass substrate, and most of the solvent was removed under vacuum at 60°C. Subsequently, the temperature was raised to 160°C to dry the film further. After removing the substrate, a free-standing, flexible, and transparent film with a thickness of *ca.* 25 μm was obtained. For optical measurement, 15 mg of Ar-PIs was dissolved in 1 ml $CHCl_3$. Then 450 μL of Ar-PIs solution was cast on a 2×2 cm^2 quartz substrate by spin coating with the condition of 2000 rpm for 1 minute. After spin coating, the substrate was heated on a hot plate at 80°C to remove the remaining solvent, resulting in a film with a thickness of *ca.* 110 nm.

Supporting Information ((delete if not applicable))

Supporting Information is available from the Wiley Online Library or from the author.

Acknowledgments

M.-C. H. and Y.-J. S. contributed equally to this work. The authors gratefully thank Prof. Jye-Shane Yang, who is in the Department of Chemistry at National Taiwan University (NTU), for assistance in the measurements of PLQY. This work is funded by the National Science and Technology Council in Taiwan (NSTC 113-2221-E-002-061-MY3 and 111-2221-E-002 -028 -MY3). The authors gratefully thank Ms. Chiu-Hui He in the Instrumentation Center at NTNU for assistance in NMR measurements and Ms. Ching-Wei Lu in the Instrumentation Center at NTU for assistance in elemental analysis measurements.

References

[1] A. Sezer Hicyilmaz, A. Celik Bedeloglu, Applications of polyimide coatings: A review, SN Applied Sciences 2021, 3, 363.

[2] a) C. Yi, W. Li, S. Shi, K. He, P. Ma, M. Chen, C. Yang, High-temperature-resistant and colorless polyimide: Preparations, properties, and applications, Solar Energy 2020, 195, 340; b) X.-J. Liu, M.-S. Zheng, G. Chen, Z.-M. Dang, J.-W. Zha, High-temperature polyimide dielectric materials for energy storage: theory, design, preparation and properties, Energy & Environmental Science 2022, 15, 56; c) A. Gumyusenge, X. Luo, Z. Ke, D. T. Tran, J. Mei, Polyimide-based high-temperature plastic electronics, ACS Materials Letters 2019, 1, 154.

[3] a) R. Bei, C. Qian, Y. Zhang, Z. Chi, S. Liu, X. Chen, J. Xu, M. P. Aldred, Intrinsic low dielectric constant polyimides: relationship between molecular structure and dielectric properties, Journal of Materials Chemistry C 2017, 5, 12807; b) Y. Li, G. Sun, Y. Zhou, G. Liu, J. Wang, S. Han, Progress in low dielectric polyimide film–A review, Progress in Organic Coatings 2022, 172, 107103.

[4] a) Y. S. Negi, S. R. Damkale, S. Ansari, Photosensitive polyimides, Journal of Macromolecular Science, Part C: Polymer Reviews 2001, 41, 119; b) X. Jin, H. Ishii, A novel positive-type photosensitive polyimide based on soluble block copolyimide showing low dielectric constant with a low-temperature curing process, Journal of Applied Polymer Science 2006, 100, 4240; c) L.-Y. Tseng, Y.-C. Lin, C.-C. Kuo, C.-C. Kuo, M. Ueda, W.-C. Chen, An ultra heat-resistant polyimide formulated with photo-base generator for alkaline-developable, negative-type photoresist, Reactive and Functional Polymers 2020, 157, 104760.

[5] a) Y. Chen, Y. Liu, Y. Min, Innovative Polyimide Modifications for Aerospace and Optoelectronic Applications: Synergistic Enhancements in Thermal, Mechanical, and Optical Properties, ACS Applied Materials & Interfaces 2025, 17, 16016; b) O. Aghababaei Tafreshi, Z. Saadatnia, S. Ghaffari-Mosanenzadeh, M. M. Rastegardoost, C. Zhang, C. B. Park, H. E. Naguib, Polyimide Aerogel Fiber Bundles for Extreme Thermal Management Systems in Aerospace Applications, ACS Applied Materials & Interfaces 2024, 16, 54597; c) Y. Zhang, S. Dai, Z. Yin, W. Yan, Q. Li, H. Yuan, X. Zhang, L. Chen, J. Luo, X. Ouyang, Integration fabrication of polyimide composite films for aerospace applications, SmartMat 2024, 5, e1225.

[6] a) H. Yu, Y. Shi, B. Yuan, Y. He, L. Qiao, J. Wang, Q. Lin, Z. Chen, E. Han, Recent developments of polyimide materials for lithium-ion battery separators, Ionics 2021, 27, 907; b) S. Cui, T. Li, D. Tao, D. Zhang, Y. Cao, F. Xu, Large Conjugated Polyimide Cathodes of Rechargeable Magnesium Batteries: Electron Delocalization Induced by Bivalent Magnesium Cations, ACS Materials Letters 2024, 6, 1883; c) F. Baskoro, S. U. Sharma, A. L. Lubis, H.-J. Yen, Recent Advances p-type Polymeric Electrode Materials towards High-Voltage 4.0 V-class Organic Lithium-ion Batteries, Journal of Materials Chemistry A 2024; d) G. Vardhini, P. S. Dilip, S. A. Kumar, S. Suriyakumar, M. Hariharan, M. M. Shaijumon, Polyimide-based aqueous potassium energy storage systems using concentrated WiSE electrolyte, ACS Applied Materials & Interfaces 2024, 16, 48782; e) F. Baskoro, A. L. Lubis, H. Q. Wong, G.-S. Liou, H.-J. Yen, Redox-active polynaphthalimides as versatile electrode materials for high-voltage, high-rate and long-cycle-life organic Li-ion batteries, Journal of Materials Chemistry A 2023, 11, 11210.

[7] M. G. Ramirez, M. Morales-Vidal, V. Navarro-Fuster, P. G. Boj, J. A. Quintana, J. M. Villalvilla, A. Retolaza, S. Merino, M. A. Díaz-García, Improved performance of perylenediimide-based lasers, Journal of Materials Chemistry C 2013, 1, 1182.

[8] a) M. Hasegawa, K. Horie, Photophysics, photochemistry, and optical properties of polyimides, Progress in Polymer Science 2001, 26, 259; b) M. Hasegawa, I. Mita, M. Kochi, R. Yokota, Charge-Transfer emission spectra of aromatic polyimides, Journal of Polymer Science Part C: Polymer Letters 1989, 27, 263; c) M. Hasegawa, M. Kochi, I. Mita, R. Yokota, Molecular aggregation and fluorescence spectra of aromatic polyimides, European Polymer Journal 1989, 25, 349.

[9] M. Hasegawa, Y. Shindo, T. Sugimura, S. Ohshima, K. Horie, M. Kochi, R. Yokota, I. Mita, Photophysical processes in aromatic polyimides. Studies with model compounds, Journal of Polymer Science Part B: Polymer Physics 1993, 31, 1617.

[10] J. Wakita, H. Sekino, K. Sakai, Y. Urano, S. Ando, Molecular design, synthesis, and properties of highly fluorescent polyimides, The Journal of Physical Chemistry B 2009, 113, 15212.

[11] H.-J. Yen, C.-J. Chen, G.-S. Liou, Novel high-efficiency PL polyimide nanofiber containing aggregation-induced emission (AIE)-active cyanotriphenylamine luminogen, Chemical Communications 2013, 49, 630.

[12] Z. Zhou, Y. Long, X. Chen, T. Yang, J. Zhao, Y. Meng, Z. Chi, S. Liu, X. Chen, M. P. Aldred, Preserving high-efficiency luminescence characteristics of an aggregation-induced emission-active fluorophore in thermostable amorphous polymers, ACS applied materials & interfaces 2020, 12, 34198.

[13] a) T. Yu, Y. Han, H. Yao, Z. Chen, S. Guan, Polymeric optoelectronic materials with low-voltage colorless-to-black electrochromic and AIE-activity electrofluorochromic dual-switching properties, Dyes and Pigments 2020, 181, 108499; b) T. Yu, P. Theato, H. Yao, H. Liu, Y. Di, Z. Sun, S. Guan, Colorless electrochromic/electrofluorochromic dual-functional triphenylamine-based polyimides: Effect of a tetraphenylethylene-based π-bridge on optoelectronic properties, Chemical Engineering Journal 2023, 451, 138441; c) T. Yu, H. Yao, H. Liu, S. Guan, High-performance fluorescent/electroactive (A4+ B2)-type hyperbranched polyimide with AIE-enhanced electroflourochromic behavior, Dyes and Pigments 2023, 214, 111207.

[14] a) Y. J. Shao, G. S. Liou, Triarylamine-Based Wholly Aromatic Polyimide with Simultaneously Unprecedented Photoluminescence Efficiency and High Glass-Transition Temperature, Advanced Optical Materials 2022, 10, 2101949; b) J.-H. Wu, W.-C. Chen, G.-S. Liou, Triphenylamine-based luminogens and fluorescent polyimides: effects of functional groups and substituents on photophysical behaviors, Polymer Chemistry 2016, 7, 1569; c) Y. Zhuang, J. G. Seong, Y. M. Lee, Polyimides containing aliphatic/alicyclic segments in the main chains, Progress in Polymer Science 2019, 92, 35.

[15] a) J.-H. Wu, G.-S. Liou, High-efficiency fluorescent polyimides based on locally excited triarylamine-containing dianhydride moieties, Polymer Chemistry 2015, 6, 5225; b) H. J. Yen, J. H. Wu, W. C. Wang, G. S. Liou, High-Efficiency Photoluminescence Wholly Aromatic Triarylamine-based Polyimide Nanofiber with Aggregation-Induced Emission Enhancement, Advanced Optical Materials 2013, 1, 668.

[16] a) J. Zhang, X. Zhao, H. Shen, J. W. Lam, H. Zhang, B. Z. Tang, White-light emission from organic aggregates: a review, Advanced Photonics 2022, 4, 014001; b) S. H. Kim, Y. Jin, J. Y. Yu, J. Kim, S. Song, H. Suh, K. Lee, Color stable white polymer light-emitting diodes with single emission layer, Synthetic metals 2010, 160, 835; c) T. Weng, G. Baryshnikov, C. Deng, X. Li, B. Wu, H. Wu, H. Ågren, Q. Zou, T. Zeng, L. Zhu, A Fluorescence–Phosphorescence–Phosphorescence Triple-Channel Emission Strategy for Full-Color Luminescence, Small 2020, 16, 1906475; d) C. Liu, H. Bai, B. He, X. He, J. Zhang, C. Chen, Y. Qiu, R. Hu, F. Zhao, Y. Zhang, Functionalization of silk by AIEgens through facile bioconjugation: full-color fluorescence and long-term bioimaging, Angewandte Chemie International Edition 2021, 60, 12424; e) L. Tu, Y.

Xie, Z. Li, B. Tang, Aggregation-induced emission: Red and near-infrared organic light-emitting diodes, SmartMat 2021, 2, 326; f) J. M. Ha, S. H. Hur, A. Pathak, J.-E. Jeong, H. Y. Woo, Recent advances in organic luminescent materials with narrowband emission, NPG Asia Materials 2021, 13, 53.

[17] O. Krupka, P. Hudhomme, Recent advances in applications of fluorescent perylenediimide and perylenemonoimide dyes in bioimaging, photothermal and photodynamic therapy, International Journal of Molecular Sciences 2023, 24, 6308.

[18] a) D.-J. Liaw, K.-L. Wang, Y.-C. Huang, K.-R. Lee, J.-Y. Lai, C.-S. Ha, Advanced polyimide materials: Syntheses, physical properties and applications, Progress in Polymer Science 2012, 37, 907; b) D. Ding, K. Li, B. Liu, B. Z. Tang, Bioprobes based on AIE fluorogens, Accounts of Chemical Research 2013, 46, 2441; c) W. Huang, D. Yan, Q. Lu, Y. Huang, Synthesis and characterization of highly soluble fluorescent main chain copolyimides containing perylene units, European Polymer Journal 2003, 39, 1099; d) S. Xu, M. Yang, S. Cao, A fluorescent copolyimide containing perylene, fluorene and oxadiazole units in the main chain, Reactive and Functional Polymers 2006, 66, 471; e) M. Fang, J. Yang, Z. Li, Light emission of organic luminogens: Generation, mechanism and application, Progress in Materials Science 2022, 125, 100914.

[19] a) J. Wakita, S. Inoue, N. Kawanishi, S. Ando, Excited-state intramolecular proton transfer in imide compounds and its application to control the emission colors of highly fluorescent polyimides, Macromolecules 2010, 43, 3594; b) K. Kanosue, T. Shimosaka, J. Wakita, S. Ando, Polyimide and imide compound exhibiting bright red fluorescence with very large stokes shifts via excited-state intramolecular proton transfer, Macromolecules 2015, 48, 1777; c) K. Kanosue, R. n. Augulis, D. Peckus, R. Karpicz, T. Tamulevičius, S. Tamulevičius, V. Gulbinas, S. Ando, Polyimide and imide compound exhibiting bright red fluorescence with very large stokes shifts via excited-state intramolecular proton transfer II. Ultrafast proton transfer dynamics in the excited state, Macromolecules 2016, 49, 1848; d) N. Liang, S. Kuwata, R. Ishige, S. Ando, Large-Stokes-shifted yellow photoluminescence emission from an imide and polyimides forming multiple intramolecular hydrogen bonds, Materials Chemistry Frontiers 2022, 6, 24.

[20] H.-J. Yen, J.-H. Wu, Y.-H. Huang, W.-C. Wang, K.-R. Lee, G.-S. Liou, Novel thermally stable and soluble triarylamine functionalized polyimides for gas separation, Polymer Chemistry 2014, 5, 4219.

[21] a) W. Li, Y. Pan, L. Yao, H. Liu, S. Zhang, C. Wang, F. Shen, P. Lu, B. Yang, Y. Ma, A hybridized local and charge-transfer excited state for highly efficient fluorescent oleds: Molecular design, spectral character, and full exciton utilization, Advanced Optical Materials 2014, 2, 892; b) R. Orita, M. Franckevičius, A. Vyšniauskas, V. Gulbinas, H. Sugiyama, H. Uekusa, K. Kanosue, R. Ishige, S. Ando, Enhanced fluorescence of phthalimide compounds induced by the incorporation of electron-donating alicyclic amino groups, Physical Chemistry Chemical Physics 2018, 20, 16033.

[22] N. J. Turro, V. Ramamurthy, J. C. Scaiano, Vol. 188, University Science Books Sausalito, CA **2010**, Ch. 6.

[23] a) S. Sasaki, G. P. Drummen, G.-i. Konishi, Recent advances in twisted intramolecular charge transfer (TICT) fluorescence and related phenomena in materials chemistry, Journal of Materials Chemistry C 2016, 4, 2731; b) C. Chen, C. Fang, Fluorescence modulation by amines: Mechanistic insights into twisted intramolecular charge transfer (TICT) and beyond, Chemosensors 2023, 11, 87.

[24] J. Mei, N. L. Leung, R. T. Kwok, J. W. Lam, B. Z. Tang, Aggregation-induced emission: together we shine, united we soar!, Chemical Reviews 2015, 115, 11718.

[25] a) Y. Luo, K. Chen, W. Wang, R. Bei, C. Li, Y. Long, Z. Zhou, S. Liu, Z. Chi, J. Xu, Synthesis and characterization of a large Stokes-shifted fluorescent imide and its related

polyimides bearing 2-(2′ -hydroxyphenyl) benzothiazole moieties, Journal of Materials Chemistry C 2023, 11, 9252; b) H. Kim, G. Kwak, Fluorescent Polyimide Films with Covalently Incorporated Perylenediimide, ACS Applied Polymer Materials 2024, 6, 7311.

[26] K. Kanosue, S. Hirata, M. Vacha, R. Augulis, V. Gulbinas, R. Ishige, S. Ando, A colorless semi-aromatic polyimide derived from a sterically hindered bromine-substituted dianhydride exhibiting dual fluorescence and phosphorescence emission, Materials Chemistry Frontiers 2019, 3, 39.

[27] L.-j. Qu, L.-s. Tang, S.-w. Liu, Z.-g. Chi, X.-d. Chen, Y. Zhang, J.-r. Xu, Preparation and photoluminescent properties of polyimides containing triphenylamine pendant group, Acta Polym Sin 2018, 11, 1430.

[28] F. Han, R. Zhang, Z. Zhang, J. Su, Z. Ni, A new TICT and AIE-active tetraphenylethene-based Schiff base with reversible piezofluorochromism, RSC Advances 2016, 6, 68178.

[29] C.-W. Chang, G.-S. Liou, Novel anodic electrochromic aromatic polyamides with multi-stage oxidative coloring based on N, N, N′ , N′ -tetraphenyl-p-phenylenediamine derivatives, Journal of Materials Chemistry 2008, 18, 5638.

[30] G.-S. Liou, H.-Y. Lin, Synthesis and electrochemical properties of novel aromatic poly (amine− amide) s with anodically highly stable yellow and blue electrochromic behaviors, Macromolecules 2009, 42, 125.

TOC figure

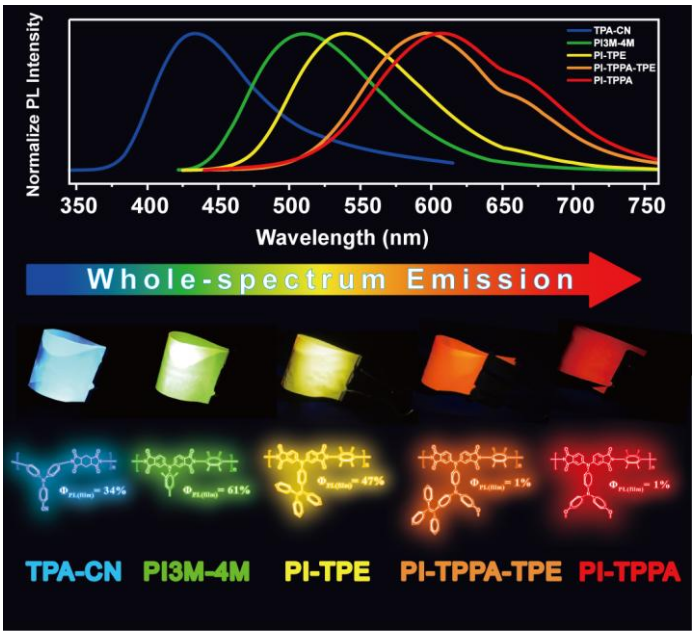

A series of triarylamine-based fluorescence polyimides with different pendant groups are designed in this work to attempt the bathochromic emission from yellow to red. **PI-TPE** results in a bathochromic shift emission at yellow emission at 540 nm with 47% quantum efficiency, and **PI-TPPA** achieves a remarkable red emission at 608 nm.